Peptoids that mimic the structure, function, and mechanism of helical antimicrobial peptides

Nathaniel P. Chongsiriwatana*, James A. Patch*†, Ann M. Czyzewski*, Michelle T. Dohm‡, Andrey Ivankin§, David Gidalevitz§, Ronald N. Zuckermann¶, and Annelise E. Barron*‡‖

Departments of *Chemical and Biological Engineering and ‡Chemistry, Northwestern University, 2145 Sheridan Road, Evanston, IL 60208; ¶Biological Nanostructures Facility, Molecular Foundry, Lawrence Berkeley National Laboratory, 1 Cyclotron Road, Berkeley, CA 94720; and §Division of Physics, Department of Biological, Chemical, and Physical Sciences, Illinois Institute of Technology, 3101 South Dearborn Street, Chicago, IL 60616

Edited by Lewis T. Williams, Five Prime Therapeutics, Emeryville, CA, and approved December 18, 2007 (received for review August 31, 2007)

Antimicrobial peptides (AMPs) and their mimics are emerging as promising antibiotic agents. We present a library of ''ampetoids'' (antimicrobial peptoid oligomers) with helical structures and biomimetic sequences, several members of which have low-micromolar antimicrobial activities, similar to cationic AMPs like pexiganan. Broad-spectrum activity against six clinically relevant BSL2 pathogens is also shown. This comprehensive structure–activity relationship study, including circular dichroism spectroscopy, minimum inhibitory concentration assays, hemolysis and mammalian cell toxicity studies, and specular x-ray reflectivity measurements shows that the *in vitro* activities of ampetoids are strikingly similar to those of AMPs themselves, suggesting a strong mechanistic analogy. The ampetoids' antibacterial activity, coupled with their low cytotoxicity against mammalian cells, make them a promising class of antimicrobials for biomedical applications. Peptoids are biostable, with a protease-resistant *N*-substituted glycine backbone, and their sequences are highly tunable, because an extensive diversity of side chains can be incorporated via facile solid-phase synthesis. Our findings add to the growing evidence that nonnatural foldamers will emerge as an important class of therapeutics.

antibiotics | peptidomimetics | structure–activity studies

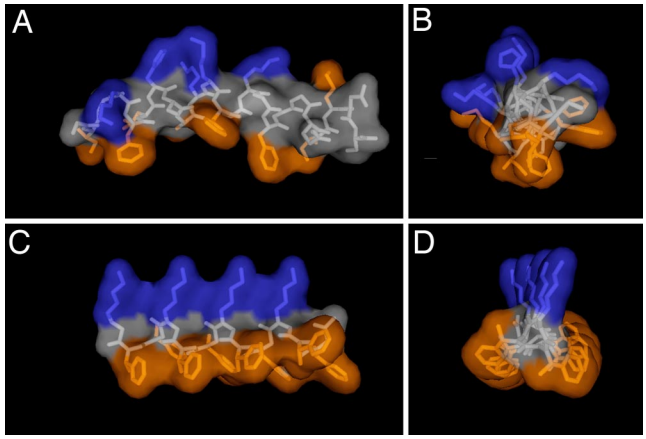

Fig. 1. NMR structure of magainin-2 in DPPC micelles [Protein Data Bank (PDB) ID Code 2MAG]. (*A* and *B*) Parallel (*A*) and perpendicular (*B*) to its helical axis. (*C* and *D*) Similar views of a model structure of ampetoid 1, using backbone ϕ and ψ angles from a published NMR structure of a peptoid helix.(37, 41) Because *N*Lys is achiral, the structure of 1 is expected to be significantly dynamic in solution. Residues are color coded: cationic, blue; hydrophobic, orange; all others, gray.

Natural antimicrobial peptides (AMPs) defend a wide array of organisms against bacterial pathogens and show potential as supplements for or replacements of conventional antibiotics, because few bacteria have evolved resistance to them (1–3). Many AMPs kill bacteria by permeabilization of the cytoplasmic membrane, causing depolarization, leakage, and death (4), whereas others target additional anionic bacterial constituents (e.g., DNA, RNA, or cell wall components) (2, 5). Amphipathic secondary structures in which residues are segregated into hydrophobic and cationic regions (Fig. 1 *A* and *B*) are the hallmark of most AMPs (6). Regardless of their final target of killing, AMPs must interact with the bacterial cytoplasmic membrane, and their amphipathicity is integral to such interactions (1, 2, 7). Additionally, their cationic nature imparts AMPs with some measure of selectivity, because mammalian cell membranes are largely zwitterionic. The precise nature of AMP–membrane interactions remains controversial and actively debated; a variety of mechanisms have been proposed, including the carpet (4), barrel-stave pore (4), toroidal pore (8), and aggregate (9) models. Nevertheless, a considerable number of structure–activity investigations have elucidated how the physicochemical properties of these molecules relate to their biological activities (4, 7, 10–22).

Although AMPs have been actively studied for decades (23–25), they have yet to see widespread clinical use (1). This is due in part to the vulnerability of many peptide therapeutics to rapid *in vivo* degradation, which dramatically reduces their bioavailability. Nonnatural mimics of AMPs can circumvent the proteolytic susceptibility of peptides while retaining their beneficial features. The short (<40-aa) cationic, linear, α-helical class of AMPs, including the well known magainins (23), are especially amenable to mimicry. β-Peptide mimics of these AMPs have been successfully created that show antibacterial and nonhemolytic *in vitro* activity (26). Poly-*N*-substituted glycines (peptoids) comprise another class of peptidomimetics that differ from peptides only in that peptoid side chains are attached to the backbone amide nitrogen rather than to the α-carbon (27), making them protease-resistant (28). More than any of the other peptidomimetic systems under study (29), including β-peptides (26, 30), β-peptoids (31), oligoureas (32), and oligo(phenylene ethynylene)s (33), peptoids (34–36) are particularly well suited for AMP mimicry because they are easily synthesized on solid phase (by using conventional peptide synthesis equipment) with access to diverse sequences at relatively low cost (27). Any chemical functionality available as a primary amine can be incorporated via a submonomer synthetic method (27); thus, peptoids are highly and finely tunable.

Author contributions: N.P.C. and J.A.P contributed equally to this work; N.P.C., J.A.P., D.G., R.N.Z., and A.E.B. designed research; N.P.C., J.A.P., A.M.C., M.T.D., and D.G. performed research; D.G. and R.N.Z. contributed new reagents/analytic tools; N.P.C., J.A.P., A.M.C., M.T.D., A.I., and D.G. analyzed data; and N.P.C., J.A.P., A.M.C., M.T.D., and A.E.B. wrote the paper.

The authors declare no conflict of interest.

This article is a PNAS Direct Submission.

†Present address: Wyeth Research, 401 North Middletown Road, Pearl River, NY 10965.

‖To whom correspondence should be sent at the present address: Department of Bioengineering, Stanford University, W300B James H. Clark Center, 318 Campus Drive, Stanford, CA 94305. E-mail: aebarron@stanford.edu.

This article contains supporting information online at www.pnas.org/cgi/content/full/0708254105/DC1.

The poly-*N*-substituted glycine structure of peptoids precludes both backbone chirality and intrachain hydrogen bonding; nevertheless, peptoids can be driven to form helical secondary structures via a periodic incorporation of bulky, α-chiral side chains (37–40). Previous work has shown that incorporation of homochiral side chains can give rise to polyproline type-I-like helices with a periodicity of approximately three monomers per turn and a helical pitch of 6.0–6.7 Å (37–39, 41, 42). The threefold periodicity of the peptoid helix facilitates the design of facially amphipathic structures similar to those formed by many AMPs; for example, the trimer repeat $(X\text{-}Y\text{-}Z)_n$ forms a peptoid helix with three faces, composed of X, Y, and Z residues.

Here, we report that the *in vitro* activities of certain antimicrobial peptoids ("ampetoids") are similar to those of many AMPs, in that ampetoids exhibit broad-spectrum antibacterial activity and low mammalian cytotoxicity. Structure–activity relationships observed in a library of rationally designed ampetoids are wholly analogous to those that describe many AMPs. Using synchrotron radiation to probe interactions between ampetoids and lipid layers, we have also found that AMP–ampetoid analogy extends to the molecular level.

Results

Initial Antibacterial Activity and Selectivity Screening. We synthesized 13 ampetoid analogs to determine whether peptoids are affected by structural and sequence modifications in a manner consistent with AMP activities (13, 17, 21, 43). The designs for ampetoids in this library were derived from two antibacterial and selective amphipathic dodecamers, **1** and **2**, from previous work (34). Peptoid **1** [H-(*N*Lys-*N*spe-*N*spe)$_4$-NH$_2$] is composed of 2/3 *N*spe, a peptoid analog of Phe, and 1/3 *N*Lys, a peptoid analog of Lys (see Fig. 1 *C* and *D* for a model structure of peptoid **1** and Fig. 2 for the structures of peptoid monomers). Peptoid **2** [H-(*N*Lys-*N*ssb-*N*spe)$_4$-NH$_2$] contains 1/3 Ile-like *N*ssb monomers in place of *N*spe. The variant sequences were designed to effect changes in chirality, length, hydrophobicity, charge, and amphipathicity. All compounds were tested for antibacterial activity against representative BSL1 Gram-negative (*Escherichia coli* JM109) and Gram-positive (*Bacillus subtilis* BR151) bacterial strains. As an initial measure of selectivity, we determined the lytic activity of the peptoids against human erythrocytes. Table 1 summarizes the sequences we synthesized, the solvent composition at RP-HPLC elution as a relative measure of molecular hydrophobicity, and antibacterial and hemolytic activities [full hemolysis curves are shown in supporting information (SI) Fig. 8]. Ten of the 15 peptoids exhibited low-micromolar MICs against both *E. coli* and *B. subtilis*, demonstrating that nonnatural peptoid oligomers can be as active as some antimicrobial peptides (MICs for pexiganan (44)—a selective AMP analog of magainin-2—and the bee-venom AMP melittin (45) are shown in Table 1).

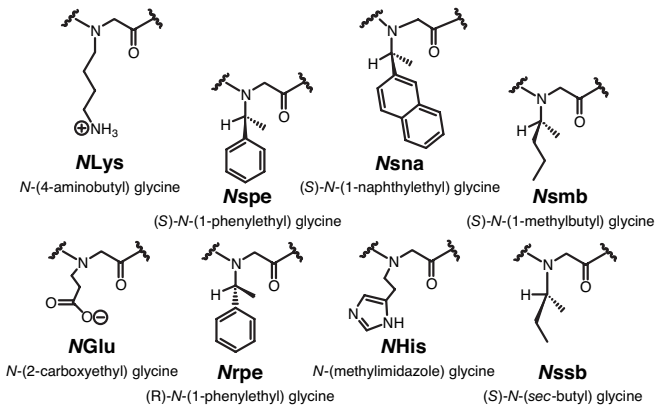

Fig. 2. Peptoid monomer side-chain structures, with full and shorthand names.

We defined the selectivity ratio (SR) (Table 1) as the quotient of the 10% hemolytic dose (HD_{10}) and the *E. coli* MIC; thus, the SR is an estimate of a compound's tendency to kill bacteria rather than mammalian cells. Ampetoid **1** had an SR of 6.0. As expected, melittin (well known to be cytotoxic) had a low SR of 1.3. Six of 13 peptoid variants were more selective than **1** (i.e., SRs >6), with SRs approaching that of pexiganan (i.e., SR of **1**-Pro$_6$ = 20, SR of pexiganan = 24).

Broad-Spectrum Antibacterial Activity Against BSL2 Bacterial Pathogens. Broad-spectrum activity against a variety of pathogenic bacteria is a hallmark of AMPs. Accordingly, we tested ampetoid

Table 1. Antibacterial and hemolytic activities of ampetoids and AMPs

Variant class	Shorthand name	Sequence	HPLC elution solvent,* %	*E. coli* MIC, μM	*B. subtilis* MIC, μM	HD_{10}/HD_{50},‡ μM	Selectivity ratio (SR)‡§
Basis	1	H-(*N*Lys-*N*spe-*N*spe)$_4$-NH$_2$	48	3.5	0.88	21/100	6.0
	2	H-(*N*Lys-*N*ssb-*N*spe)$_4$-NH$_2$	39	31	3.9	>120/>120	>3.9
Chirality	$1_{enantiomer}$	H-(*N*Lys-*N*rpe-*N*rpe)$_4$-NH$_2$	48	3.5	0.88	16/86	4.6
Length	1_{6mer}	H-(*N*Lys-*N*spe-*N*spe)$_2$-NH$_2$	41	27	27	>220/>220	>8.1
	1_{9mer}	H-(*N*Lys-*N*spe-*N*spe)$_3$-NH$_2$	46	9.1	1.2	>150/>150	>16
	1_{15mer}	H-(*N*Lys-*N*spe-*N*spe)$_5$-NH$_2$	51	5.5	1.4	3/19	0.55
Hydrophobicity	2-*N*smb$_{2,5,8,11}$	H-(*N*Lys-*N*smb-*N*spe)$_4$-NH$_2$	48	7.4	0.95	>120/>120	>16
	2-*N*sna$_{6,12}$	H-(*N*Lys-*N*ssb-*N*spe-*N*Lys-*N*ssb-*N*sna)$_2$-NH$_2$	47	7.2	0.93	55/>120	7.6
	1-*N*sna$_{6,12}$	H-(*N*Lys-*N*spe-*N*spe-*N*Lys-*N*spe-*N*sna)$_2$-NH$_2$	53	3.3	1.6	4/22	1.2
	1-*N*His$_{6,12}$	H-(*N*Lys-*N*spe-*N*spe-*N*Lys-*N*spe-*N*His)$_2$-NH$_2$	37	3.5	6.9	>110/>110	>31
	1-Pro$_6$	H-*N*Lys-*N*spe-*N*spe-*N*Lys-*N*spe-L-Pro-(*N*Lys-*N*spe-*N*spe)$_2$-NH$_2$	40	3.1	1.6	63/>110	20
Charge	1-*N*Glu$_{4,10}$	H-(*N*Lys-*N*spe-*N*spe-*N*Glu-*N*spe-*N*spe)$_2$-NH$_2$	60†	>110	6.9	19/40	<0.17
	1-*N*Glu$_{1,4,7,10}$	H-(*N*Glu-*N*spe-*N*spe)$_4$-NH$_2$	54†	>219	>219	>110/>110	N/A
Amphipathicity	1_{block}	H-(*N*Lys)$_4$-(*N*spe)$_8$-NH$_2$	54	6.9	1.7	18/73	2.6
	$2_{scrambled}$	H-*N*Lys-*N*ssb-*N*spe-*N*ssb-*N*spe-*N*Lys-*N*spe-*N*Lys-*N*ssb-*N*ssb-*N*spe-*N*Lys-NH$_2$	42	31	15	>120/>120	>3.9
AMPs	Pexiganan	GIGKFLKKAKKFGKAFVKILKK-NH$_2$	38	3.1	1.6	73/>200	24
	Melittin	GIGAVLKVLTTGLPALISWIKRKRQQ-NH$_2$	54	1.6	0.78	2/6	1.3

*Percent acetonitrile in water, 0.1% (vol/vol) trifluoroacetic acid (TFA) at HPLC elution.
†With 10 mM ammonium acetate and no TFA (pH 7.0).
‡For concentrations reported as "> *x*", *x* = 200 μg/ml—the highest concentration tested (except for pexiganan, which was tested up to 500 μg/ml).
§Selectivity ratio, SR = (HD_{10})/(*E. coli* MIC).

Table 2. Broad-spectrum activity of 1 against BSL2 CLSI quality control strains, compared to MICs of pexiganan as determined by Ge *et al.* (44)

Microorganism	Clinical relevance	Peptoid 1 MIC, μM	Pexiganan MIC, μM
Streptococcus pneumoniae ATCC 49619	Leading cause of community-acquired pneumonia	1.7–3.4	13
Haemophilus influenzae ATCC 49247	Second-most common cause of community-acquired pneumonia	6.9	3.2
Staphylococcus aureus ATCC 33591	Leading cause of antibiotic-resistant nosocomial infection. This strain is methicillin resistant.	3.4	6.5–13
Escherichia coli ATCC 25922	Common Gram-negative pathogen	14–28	3.2–6.5
Enterococcus faecalis ATCC 29212	*E. faecalis* has evolved resistance to the toughest of antibiotics (e.g. vancomycin)	3.4–6.9	26
Pseudomonas aeruginosa ATCC 27853	Highly unresponsive to many antibiotic treatments	28	3.2–6.5

1 against six clinically relevant biosafety-level-2 (BSL2) bacterial pathogens. The MICs for these microorganisms, summarized in Table 2, demonstrated promising activity, comparable with that of pexiganan, which was optimized for pharmaceutical applications (44).

Ampetoid Selectivity Evaluated by Using Cultured Mammalian Cells. We evaluated the biocompatibility of selected oligomers with A549 lung epithelial cells by using the MTS assay (46). Fig. 3 shows that the 10% metabolic inhibitory dose (ID_{10}) and 50% inhibitory dose (ID_{50}) of these selected peptoids compared favorably to that of pexiganan and melittin; ampetoids **1**-Pro_6 and **1**-$NHis_{6,12}$, with MICs <7 μM, had ID_{10}s 10 and 20 times that of pexiganan. Interestingly, nonselective peptoid $\mathbf{1}_{15mer}$ exhibited cytotoxicity no worse than pexiganan.

Structure–Activity Studies. Structure–activity relationships derived from our library of ampetoids are discussed below, according to the primary physicochemical parameter that was altered. We used circular dichroism (CD) spectroscopy to compare the helicities of the ampetoids by monitoring the intensity of spectral extrema, particularly at 190 and 220 nm (37–39, 41, 42, 47). We performed CD in 10 mM aqueous Tris buffer (pH 7.4), alone and in the presence of two types of small unilamellar vesicles (SUVs) composed of model binary lipid mixtures: (*i*) anionic *E. coli* membrane-mimetic SUVs [POPE/POPG (7:3 mole ratio)] (48) and (*ii*) zwitterionic erythrocyte membrane-mimetic SUVs [POPC/cholesterol (CH) (1:1 mole ratio)] (49).

Chirality. Using enantiomeric side chains (*N*rpe in place of *N*spe; Fig. 2) (42), we created a left-handed helical analog of **1**, called $\mathbf{1}_{enantiomer}$, as evidenced by its mirror-image CD spectrum compared with that of **1** (Fig. 4A) (47). The activities and selectivities of **1** and $\mathbf{1}_{enantiomer}$ were congruent (Table 1).

Length. We created length variants of **1** ranging from 6 to 15 monomers, all with the same threefold sequence repeat and 1:3 charge-to-length ratio. The shortened variants, $\mathbf{1}_{6mer}$ and $\mathbf{1}_{9mer}$ (≈12 Å and 18 Å in length, respectively), were both active antimicrobials and more selective than **1** (Table 1). The lengthened variant, $\mathbf{1}_{15mer}$ (≈30 Å in length), was substantially more hemolytic (SR = 0.55) and cytotoxic (Fig. 3) than **1** and slightly less antibacterial. The helicities of these compounds in buffer were congruent (SI Fig. 9).

Hydrophobicity. We modulated hydrophobicity independently of length by replacing hydrophobic Ile-like *N*ssb and Phe-like *N*spe monomers in **1** and **2** with bulkier and more hydrophobic *N*smb and *N*sna, respectively (Fig. 2). The heightened molecular hydrophobicity of **2**-$Nsmb_{2,5,8,11}$ and **2**-$Nsna_{6,12}$ led to increases in both antibacterial and hemolytic activities (Table 1 and SI Fig. 8*B*). **1**-$Nsna_{6,12}$, however, showed no enhancement of antibacterial activity relative to **1**, but was much more hemolytic (SR = 1.2) (SI Fig. 8*B*).

We also created two variants of **1** with reduced hydrophobicity. Two evenly spaced hydrophobic *N*spe residues in **1** were replaced by *N*His, an achiral peptoid analog of histidine (Fig. 2) that is polar yet predominantly uncharged at physiological pH, yielding **1**-$NHis_{6,12}$. This oligomer exhibited substantially decreased *in vitro* hemolysis (SR >31; Table 1) and decreased cytotoxicity (Fig. 3), with only a slight reduction in antibacterial activity against *B. subtilis* compared with **1**. A second reduced-hydrophobicity variant, **1**-Pro_6, was created by replacing the *N*spe at position 6 with L-proline. Although Pro is well known to destabilize peptide α-helices, **1**-Pro_6 and **1** were similarly helical in buffer (Fig. 4*A*) because l-Pro is well accommodated in right-handed type-I-polyproline-like peptoid helices (SI Fig. 10). **1**-Pro_6 (SR = 24) exhibited less hemolysis and less cytotoxicity than **1**, with similar antibacterial activity (Table 1, Fig. 3).

Charge. We substituted *N*Lys monomers in **1** with glutamate-like *N*Glu (Fig. 2) to create **1**-$NGlu_{4,10}$ and **1**-$NGlu_{1,4,7,10}$. Zwitterionic **1**-$NGlu_{4,10}$ had significantly reduced activity against *B. subtilis* compared with **1** and was inactive against *E. coli* (Table 1), likely because of the absence of favorable electrostatic interactions with anionic bacterial membranes; however, it was quite hemolytic (SR <0.17). The fully anionic variant, **1**-$NGlu_{1,4,7,10}$ was devoid of both antibacterial and hemolytic activity.

Amphipathicity. We created a terminally, rather than facially, amphipathic isomer of **1** with block-like architecture ($\mathbf{1}_{block}$), and a scrambled sequence of **2** designed to preclude global amphipathicity ($\mathbf{2}_{scrambled}$) (Table 1). The terminal segregation of cationic and hydrophobic residues in the $\mathbf{1}_{block}$ sequence ensures a strongly

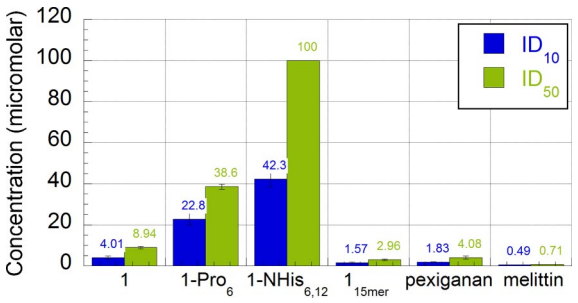

Fig. 3. Cytotoxicity data for selected peptoids and comparator peptides against A549 lung epithelial cells.

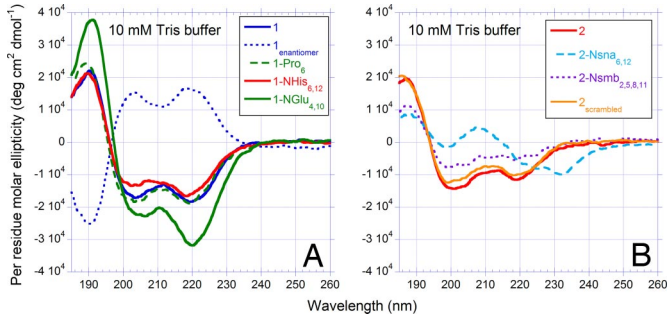

Fig. 4. CD spectra of variants of **1** (*A*) and variants of **2** (*B*) in 10 mM Tris buffer (pH 7.4).

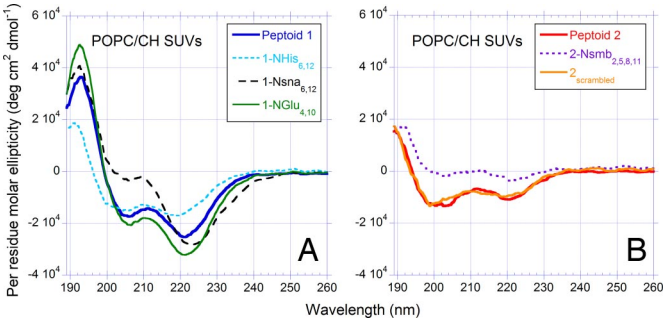

Fig. 5. CD spectra of variants of **1** (*A*) and variants of **2** (*B*) in 5 mM POPC/cholesterol (1:1) SUVs suspended in 10 mM Tris buffer (pH 7.4).

amphipathic structure independent of the facial organization of residues along a helix. $\mathbf{1}_{\text{block}}$ was slightly less antibacterial and more hemolytic than **1** (SR = 2.6), although it has the same monomer composition. The CD spectra of $\mathbf{2}_{\text{scrambled}}$ in buffer and lipid environments (Figs. 4*B*, 5*B*, and 6*B*) were nearly congruent to those of **2,** suggesting that $\mathbf{2}_{\text{scrambled}}$ forms a structured helix that, because of its scrambled sequence, has low global amphipathicity relative to **2**. Peptoid $\mathbf{2}_{\text{scrambled}}$ exhibited antibacterial activity but no hemolysis up to 120 μM.

X-Ray Reflectivity Studies of Ampetoid Orientation in Lipid Layers. We carried out liquid (aqueous buffer) surface specular x-ray reflectivity (XR) studies using synchrotron radiation to investigate the membrane orientation and depth of penetration of ampetoid **1** in a model lipid layer that mimics the outer leaflet of the cell membrane (Fig. 7) (50, 51). X-rays reflected off of the monolayer yielded an electron density profile perpendicular to the interface, allowing determination of the layer thickness and the presence and orientation of added molecules. The experimental data were represented as a stack of slabs, each with a uniform thickness, electron density, and interface roughness (52).

XR data for a pure DPPG (anionic) film (Fig. 7, circles) fit well with a two-slab model, yielding a hydrocarbon tail density (ρ_t/ρ_s) of 0.99 and a hydrocarbon tail slab thickness (L_1) of 17.9 Å as well as a head-group electron density (ρ_h/ρ_s) of 1.54 and head-group slab thickness (L_2) of 5.7 Å. These data are in good agreement with previous DPPG monolayer x-ray work (51). The XR profile changed dramatically after **1** was introduced (Fig. 7, squares) and fit a four-slab model corresponding to (*i*) lipid tails without **1** (ρ_t/ρ_s = 0.96, L_1 = 12.1 Å), (*ii*) lipid tails with partial insertion of **1** (ρ_{t+p}/ρ_s = 1.05, L_2 = 2.8 Å), (*iii*) lipid headgroups with **1** fully inserted (ρ_{h+p}/ρ_s = 1.33, L_2 = 7.0 Å), and (*iv*) peptoid **1** alone, protruding beyond the DPPG head groups (ρ_p/ρ_s = 1.16, L_2 = 3.6 Å). This electron density profile was consistent with insertion of **1** through the lipid head groups and partially into the lipid tail region.

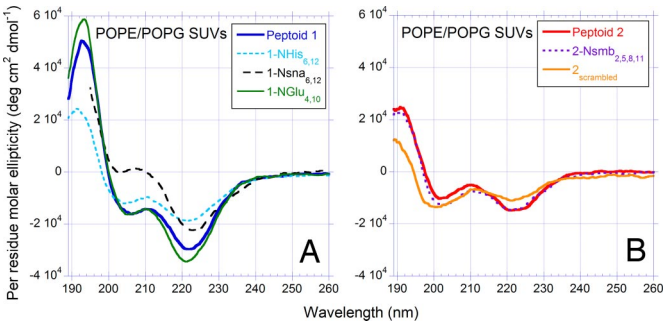

Fig. 6. CD spectra of variants of **1** (*A*) and variants of **2** (*B*) in 5 mM POPE/POPG (7:3) SUVs suspended in 10 mM aqueous Tris buffer (pH 7.4).

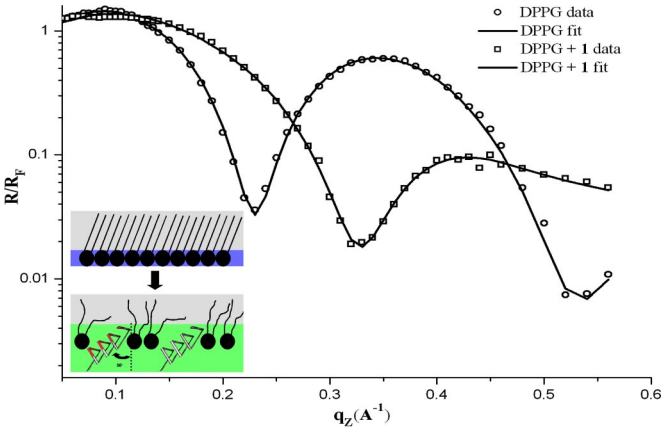

Fig. 7. X-ray reflectivity data and corresponding fit for DPPG monolayer before (circles; *Inset Upper*) and after (squares; *Inset Lower*) peptoid 1 was injected into the subphase.

Assuming that **1** retained its helical structure in the monolayer, the data suggest that **1** inserted at an angle of ≈56° between the interface normal and the long helical axis of the peptoid.

Discussion

Previous work has shown that peptoids can be used to create compounds with antimicrobial activities similar to AMPs (34). In this study, we exploited the facile synthesis and high propensity for helix formation of certain peptoids to create and study a library of ampetoid variants that suggests strong functional and mechanistic analogy between ampetoids and AMPs and that demonstrates the ampetoids' potential for development into clinically useful antibiotics.

The equivalent activities of **1** and $\mathbf{1}_{\text{enantiomer}}$ demonstrate that ampetoid mechanism does not depend on overall handedness or on stereospecific interactions with receptors or enzymes, an attribute that has also been observed for many AMPs (43). Evidence that ampetoids interact with and insert into membranes is provided by x-ray reflectivity studies (Fig. 7). Furthermore, the depth of insertion of peptoid **1**—through the head groups and partially into the lipid tails—demonstrates that **1** interacts simultaneously with hydrophobic and hydrophilic lipid moieties; thus, as with AMPs, the amphipathic structure of **1** is integral to its interactions with membranes. The orientation of **1** at an angle of ≈56° to the interface normal suggests that **1** does not operate through a barrel-stave mechanism, because that would require a transmembrane configuration (5). Although it cannot be concluded that **1** exhibits identical mechanistic behavior to natural, α-helical antimicrobial peptides, these x-ray results demonstrate ampetoid-lipid interactions consistent with those seen for AMPs such as pexiganan (53) and LL-37 (51).

We have found that ampetoid activity also adheres to trends relating structure and function in a manner analogous to AMPs—physicochemical properties of selective ampetoids are consistent with those of selective AMPs and nonselective peptoids exhibit close similarities to cytotoxic AMPs. Numerous structure–activity studies of a wide variety of AMPs have delineated the physicochemical characteristics that give rise to selective antibacterial activity or nonselective cytotoxicity. Regardless of structural class (i.e., α-helix, β-sheet, loop, or extended), nonselective AMPs typically (*i*) are very hydrophobic, such that their interactions with membranes are governed primarily by the hydrophobic effect (10–15), and (*ii*) have a well defined amphipathic structure (4, 11, 14–17). In contrast, the antibacterial activity of selective AMPs depends on (*i*) high net cationic charge (12–14, 18) (although excessive cationic charge can also lead to hemolytic activity) (18, 19)

and (*ii*) only moderate hydrophobicity (16, 19, 21, 22). Perhaps counterintuitively, a well defined amphipathic structure is not necessary for selective antimicrobial activity (7, 16); destabilization of AMP secondary structure often leads to improvements in selectivity (15, 20).

In our library, **1**-*N*Glu$_{4,10}$, **1**$_{15mer}$, **1**-*N*sna$_{6,12}$, and **1**$_{block}$ were all less selective than peptoid **1** (SRs <6.0) (Table 1). Consistent with properties of nonselective AMPs, these compounds are all either more hydrophobic (according to RP-HPLC elution time) and/or less charged (**1**-*N*Glu$_{4,10}$) than **1**. Furthermore, they are all as (or more) helical than **1** in erythrocyte-mimetic POPC/CH SUVs (Fig. 5), indicative of their well defined membrane-bound amphipathic structures in that lipid environment.

In contrast, **1**$_{9mer}$, **1**-*N*His$_{6,12}$, and **1**-Pro$_6$ all had antibacterial activities comparable to **1**, but enhanced selectivities (SRs >6.0). These peptoids are all more hydrophilic than **1**, and all have a net charge of at least +3. Thus, ampetoids are selectively active provided they have a net positive charge and are sufficiently but not excessively hydrophobic, consistent with observations of selective AMPs (4, 11). Additionally, retention of antibacterial activity and enhancement of selectivity in the shortened **1**$_{9mer}$ is analogous to behavior observed in studies of truncated AMPs (10, 16, 21, 22).

The effect of length on ampetoid potency and selectivity can largely be attributed to differences in hydrophobicity (RP-HPLC retention time, Table 1), which increases proportionally with length. Because the 12mer **1** was more antibacterial than longer and shorter analogs, these results suggest the existence of an optimal hydrophobicity at which antibacterial activity is maximized; added hydrophobicity increases only hemolytic activity. This conclusion is also supported by the hydrophobicity variants, because moderately hydrophobic **2**-*N*smb$_{2,5,8,11}$ and **2**-*N*sna$_{6,12}$ are both more antibacterial and more hemolytic than **2**, whereas the strongly hydrophobic **1**-*N*sna$_{6,12}$ (Table 1 and SI Fig. 8*B*) shows enhancement of hemolytic but not antibacterial activity relative to **1** (additional discussion in *SI Text*).

Although they are more hemolytic than **2,** peptoids **2**-*N*sna$_{6,12}$ and **2**-*N*smb$_{2,5,8,11}$ are still more selective (SRs of 7.6 and 16, respectively) than **1**, and their physicochemical properties are consistent with this finding. They are highly charged (+4), moderately hydrophobic, and exhibit CD spectra consistent with low helicity (Figs. 4*B*, 5*B*, and 6*B*). In general, CD spectra in erythrocyte-mimetic POPC/CH SUVs (Fig. 5) reveal a correlation between hemolytic activity and helicity. **1**-*N*sna$_{6,12}$, and **1**-*N*Glu$_{4,10}$ are the most hemolytic ampetoids (Table 1 and SI Fig. 8) and are the most helical in POPC/CH SUVs (Fig. 5*A*). Conversely, **1**-*N*His$_{6,12}$, **2**, **2**-*N*smb$_{6,12}$, and **2**$_{scrambled}$ are less hemolytic (Table 1 and SI Fig. 8), and less helical (Fig. 5) than **1**.

CD spectra of ampetoids in bacteria-mimetic POPE/POPG SUVs (Fig. 6), however, show that the extent of helicity is poorly correlated with antimicrobial activity. For example, **1**-*N*sna$_{6,12}$ is less helical than **1** (Fig. 6*A*), but the two compounds have similar antibacterial potencies (Table 1). Also, **2**-*N*smb$_{2,5,8,11}$ is similarly helical to **2** (Fig. 6*B*), yet **2**-*N*smb$_{2,5,8,11}$ is much more antibacterial (Table 1). Together, these results suggest that a defined helical structure is important only as a means to organize an amphipathic structure and is required for hemolytic, but not antibacterial, activity. Based on this conclusion, **1**$_{block}$, which has a well defined terminally amphipathic structure independent of its helicity, should be hemolytic, and it is (SR = 2.6). Likewise, a helical but poorly amphipathic compound such as **2**$_{scrambled}$ should be antimicrobial, but selective; indeed, **2**$_{scrambled}$ kills bacteria, but exhibits no hemolysis up to 120 μM.

In summary, these results suggest that antibacterial activity among AMPs and ampetoids alike depends on moderate hydrophobicity and net cationic charge, whereas hemolytic activity is associated primarily with high hydrophobicity and a strongly amphipathic structure, regardless of helical content. The relationships between structure and function in ampetoids are empirically analogous to those in AMPs. X-ray reflectivity studies, which show that ampetoid **1** is membrane-active and adopts a stable membrane-bound orientation, demonstrate molecular-level analogy between AMPs and ampetoids.

As both structural and functional mimics of AMPs, ampetoids act via mechanisms similar to those that have been refined over the course of evolution; thus, much of the knowledge amassed in the AMP field should be transferable to the development of peptoid antibiotics. Peptoids have greater potential than peptides to be used as pharmaceuticals and in biomaterials because of their improved stability, bioavailability, and highly tunable side-chain chemistry. Because peptides' potential for toxicity is a major obstacle limiting their clinical use (1), ampetoids' low cytotoxicity observed here relative to the AMP pexiganan further emphasizes their therapeutic potential. The results reported herein will aid in the rational design and optimization of ampetoids and other nonnatural oligomers as antimicrobials in the future.

Materials and Methods

Synthesis and Purification. Peptoids were synthesized on an ABI 433A peptide synthesizer or a parallel synthesis robot on Rink amide resin according to the submonomer method (27, 54). Briefly, the amide on the nascent chain is bromoacetylated, followed by S_N2 displacement of bromide by a primary amine to form the side chain (see *SI Text* for amines used). Peptides were synthesized by using standard Fmoc chemistry. After synthesis, oligomers were cleaved and deprotected in trifluoroacetic acid (TFA)/triisopropylsilane/water (95:2.5:2.5 by vol.) for 10 min. Compounds were purified to >97% homogeneity by RP-HPLC on a C18 column with a linear acetonitrile/water (0.1% TFA) gradient. Mass spectrometry was used to confirm the molecular weight of the purified product.

SUV Preparation. Lipid mixtures, either POPE/POPG (7:3) or POPC/CH (1:1), were dissolved in chloroform, dried under N_2, and lyophilized overnight. The lipid film was hydrated with 10 mM Tris·HCl (pH 7.4) at 40°C for 1 h. The resulting multilamellar vesicle suspension was vortexed and then sonicated at 40°C until the solution clarified to make SUVs, which were used within 6 h.

CD Spectroscopy. CD measurements were performed on a Jasco 715 spectropolarimeter, by using a quartz cylindrical cell (path length = 0.02 cm), with 50 μM peptoid in 10 mM Tris·HCl (pH 7.4) and 5 mM lipids when SUVs were used. Scans were conducted at 100 nm/min between 185 and 280 nm with 0.2-nm data pitch, 1-nm bandwidth, 2-s response, 100-mdeg sensitivity, and 40 accumulations.

Antibacterial Assays. MICs were determined according to CLSI M7-A6 protocols in a 96-well microtiter plate. In test wells, 50 μl of bacterial inoculum (1×10^6 CFU/ml) in Mueller–Hinton broth (MHB) was added to 50 μl of peptoid solution in MHB (prepared by 1:2 serial dilutions). Positive controls contained 50 μl of inoculum and 50 μl of MHB without peptoid. The MIC was defined as the lowest concentration of peptoid that completely inhibited bacterial growth after incubation at 35°C for 16 h. MIC values reported were reproducible between three independent experimental replicates, each consisting of two parallel trials. Broad-spectrum MIC testing was performed against BSL2 pathogens by Nova Biologicals.

Hemolysis Assays. Erythrocytes were isolated from freshly drawn, heparanized human blood and resuspended to 20 vol% in PBS (pH 7.4). In a 96-well microtiter plate, 100 μl of erythrocyte suspension was added to 100 μl of peptoid solution in PBS (prepared by 1:2 serial dilutions) or 100 μl of PBS in the case of negative controls. One-hundred percent hemolysis wells contained 100 μl of blood cell suspension with 100 μl of 0.2 vol% Triton X-100. The plate was incubated for 1 h at 37°C, and then each well was diluted with 150 μl of PBS. The plate was then centrifuged at 1,200 $\times$ *g* for 15 min, 100 μl of the supernatant from each well was transferred to a fresh microtiter plate, and A_{350} was measured. Percentage of hemolysis was determined as $(A - A_0)/(A_{total} - A_0) \times 100$, where A is the absorbance of the test well, A_0 the absorbance of the negative controls, and A_{total} the absorbance of 100% hemolysis wells, all at 350 nm.

MTS Assays. A549 carcinoma-derived lung epithelial cells (CCL-185; American Type Culture Collection) were cultured in Ham's F12K media. A peptoid solution plate (100 μl per well) was prepared by serial dilution of aqueous peptoid stocks in media. Peptoid solutions were transferred to a 96-well plate of day-old cell monolayers containing 100 μl per well media with ≈5,000 cells per well. MTS reagent (Promega) (40 μl per well) was added to each well, and the plate was

incubated at 37°C for 3 h, after which absorbance at 490 nm was read. Percentage of inhibition = $[1 - (A - A_{testblank})/(A_{control} - A_{blank})] \times 100$, where A is the absorbance of the test well and $A_{control}$ the average absorbance of wells with cells exposed to media and MTS (no peptoid). $A_{testblank}$ (media, MTS, and peptoid) and A_{blank} (media and MTS) were background absorbances measured in the absence of cells. The average of six replicates are reported.

Specular X-Ray Reflectivity. XR experiments were carried out at the 9-ID beamline at the Advanced Photon Source, Argonne National Laboratory (Argonne, IL). The custom-built Langmuir trough was mounted in a He-filled, sealed canister and equipped with a moveable single barrier. The surface pressure was measured by using a Wilhelmy plate. Constant-pressure insertion experiments were performed at room temperature on Dulbecco's PBS (D-PBS) subphase. DPPG (Avanti Polar Lipids) was dissolved to a known concentration in 65/35 (vol/vol) chloroform/methanol, then spread at the air–buffer interface by using a glass syringe; organic solvent was allowed to evaporate for 10 min. The monolayer was compressed to the surface pressure thought to occur in cell membranes, 30 mN/m, and XR was performed on the pure lipid layer. Then, peptoid **1** dissolved in D-PBS was injected into the subphase to a total concentration of 6.3 μM (twice the *E. coli* MIC), and allowed to insert for ≈45 min, after which XR measurements were again collected. The x-ray reflectivity (XR) profile was determined by the Fourier transform of the gradient of the electron density perpendicular to the interface. XR measurements were carried out over a range of angles corresponding to q_z values of ≈0–0.6 Å^{-1}, where $q_z = (4\pi/\lambda)\sin(\alpha)$, λ is the wavelength, and α is the angle.

ACKNOWLEDGMENTS. We thank Dr. David M. Steinhorn for hemolysis assays, Chao Liu and Ivan Kuzmenko for x-ray studies, Pamela Focia for model structure of peptoid **1**, Joanna Burdette for cell culture, and Phillip B. Messersmith for helpful comments. N.P.C. was supported by a Department of Homeland Security Fellowship. J.A.P. was supported by National Institutes of Health (NIH) National Research Service Award Molecular Biophysics Training Grant 5 T32 GM08382-10. A.M.C. was supported by a 3M graduate research fellowship. A.E.B. acknowledges support from Northwestern University's Institute for Bioengineering and Nanoscience in Advanced Medicine, the Dreyfus Foundation, a DuPont Young Investigator award, NIH Grants 1 R01 HL67984 and 1 R01 AI072666, and National Science Foundation Grant L474530-A2//CHE-0404704. Work at the Molecular Foundry was supported by the Office of Science, Office of Basic Energy Sciences, of the U.S. Department of Energy under Contract DE-AC02-05CH11231.

1. Hancock RE, Sahl HG (2006) *Nat Biotechnol* 24:1551–1557.
2. Jenssen H, Hammill P, Hancock REW (2006) *Clin Microbiol Rev* 19:491–511.
3. Peschel A, Sahl, H-G (2006) *Nat Rev Microbiol* 4:529–536.
4. Shai Y (2002) *Biopolymers (Peptide Sci)* 66:236–248.
5. Brogden KA (2005) *Nat Rev Microbiol* 3:238–250.
6. Zasloff M (2002) *Nature* 415:389–395.
7. Pag U, Oedenkoven M, Papo N, Oren Z, Shai Y, Sahl HG (2004) *J Antimicrob Chemother* 53:230–239.
8. Matsuzaki K (1998) *Biochim Biophys Acta* 1376:391–400.
9. Wu M, Maier E, Benz R, Hancock REW (1999) *Biochemstry* 38:7235–7242.
10. Blondelle SE, Houghten RA (1992) *Biochemistry* 31:12688–12694.
11. Chen Y, Mant CT, Farmer SW, Hancock REW, Vasil ML, Hodges RS (2005) *J Biol Chem* 280:12316–12329.
12. Frecer V (2006) *Bioorg Med Chem* 14:6065–6074.
13. Maloy WL, Kari UP (1995) *Biopolymers* 37:105–122.
14. Park Y, Kim HN, Park SN, Jang SH, Choi CH, Lim HT, Hahm KS (2004) *Biotechnol Lett* 26:493–498.
15. Shin SY, Lee SH, Yang ST, Park EJ, Lee DG, Lee MK, Eom SH, Song WK, Kim Y, Hahm KS, *et al.* (2001) *J Peptide Res* 58:504–514.
16. Bessalle R, Gorea A, Shalit I, Metzger JW, Dass C, Desiderio DM, Fridkin M (1993) *J Med Chem* 36:1203–1209.
17. Shai Y, Oren Z (2001) *Peptides* 22:1629–1641.
18. Bessalle R, Haas H, Goria A, Shalit I, Fridkin M (1992) *Antimicrob Agents Chemother* 36:313–317.
19. Dathe M, Nikolenko H, Meyer J, Beyermann M, Bienert M (2001) *FEBS Lett* 501:146–150.
20. Song YM, Yang ST, Lim SS, Kim Y, Hahm KS, Kim JI, Shin SY (2004) *Biochem Biophys Res Commun* 314:615–621.
21. Feder R, Dagan A, Mor A (2000) *J Biol Chem* 275:4230–4238.
22. Kustanovich I, Shalev DE, Mikhlin M, Gaidukov L, Mor A (2002) *J Biol Chem* 277:16941–16951.
23. Zasloff M (1987) *Proc Natl Acad Sci USA* 84:5449–5453.
24. Ganz T, Selsted ME, Szklarek D, Harwig SS, Daher K, Bainton DF, Lehrer RI (1985) *J Clin Invest*, 76:1427–1435.
25. Payne JW, Jakes R, Hartley BS (1970) *Biochem J* 117:757–766.
26. Porter EA, Weisblum B, Gellman SH (2002) *J Am Chem Soc* 124:7324–7330.
27. Zuckermann RN, Kerr JM, Kent SBH, Moos WH (1992) *J Am Chem Soc* 114:10646–10647.
28. Miller SM, Simon RJ, Ng S, Zuckermann RN, Kerr JM, Moos WH (1994) *Bioorg Med Chem Lett* 4:2657–2662.
29. Gante J (1994) *Angew Chem Int Ed* 33:1699–1720.
30. Seebach D, Overhand M, Kuhnle FNM, Martinoni B, Oberer L, Hommel U, Widmer H (1996) *Helv Chim Acta* 79:913–941.
31. Hamper BC, Kolodziej SA, Scates AM, Smith RG, Cortez E (1998) *J Org Chem* 63:708–718.
32. Violette A, Averlant-Petit MC, Semetey V, Hemmerlin C, Casimir R, Graff R, Marraud M, Briand, J-P, Rognan D, Guichard G (2005) *J Am Chem Soc* 127:2156–2164.
33. Arnt L, Tew GN (2002) *J Am Chem Soc* 124:7664–7665.
34. Patch JA, Barron AE (2003) *J Am Chem Soc* 125:12092–12093.
35. Seurynck SL, Patch JA, Barron AE (2005) *Chem Biol* 12:77–88.
36. Statz AR, Meagher RJ, Barron AE, Messersmith PB (2005) *J Am Chem Soc* 127:7972–7973.
37. Wu CW, Sanborn TJ, Huang K, Zuckermann RN, Barron AE (2001) *J Am Chem Soc* 123:6778–6784.
38. Wu CW, Kirshenbaum K, Sanborn TJ, Patch JA, Huang K, Dill KA, Zuckermann RN, Barron AE (2003) *J Am Chem Soc* 125:13525–13530.
39. Armand P, Kirshenbaum K, Falicov A, Dunbrack RL, Dill KA, Zuckermann RN, Cohen FE (1997) *Folding Design* 2:369–375.
40. Sanborn TJ, Wu CW, Zuckerman RN, Barron AE (2002) *Biopolymers* 63:12–20.
41. Armand P, Kirshenbaum K, Goldsmith RA, Farr-Jones S, Barron AE, Truong KTV, Dill KA, Mierke DF, Cohen FE, Zuckermann RN, *et al.* (1998) *Proc Natl Acad Sci USA* 95:4309–4314.
42. Kirshenbaum K, Barron AE, Goldsmith RA, Armand P, Bradley EK, Truong KTV, Dill KA, Cohen FE, Zuckermann RN (1998) *Proc Natl Acad Sci USA* 95:4303–4308.
43. Bessalle R, Kapitkovsky A, Gorea A, Shalit I, Fridkin M (1990) *FEBS Lett* 274:151–155.
44. Ge YG, MacDonald DL, Holroyd KJ, Thornsberry C, Wexler H, Zasloff M (1999) *Antimicrob Agents Chemother* 43:782–788.
45. Fennell JF, Shipman WH, Cole LJ (1968) *Proc Soc Exp Biol Med* 127:707–710.
46. Mosmann T (1983) *J Immunol Methods* 65:55–63.
47. Wu CW, Sanborn TJ, Zuckermann RN, Barron AE (2001) *J Am Chem Soc* 123:2958–2963.
48. Kruijff BD, Killian JA, Rietveld AG, Kusters, R (1997) in *Lipid Polymorphism and Membrane Properties*, ed Epand RM (Academic, London), Vol 44.
49. Dodge JT, Phillips GB (1967) *J Lipid Res* 8:667–675.
50. Gidalevitz D, Ishitsuka YJ, Muresan AS, Konovalov O, Waring AJ, Lehrer RI, Lee KYC (2003) *Proc Natl Acad Sci USA* 100:6302–6307.
51. Neville F, Cahuzac M, Konovalov O, Ishitsuka Y, Lee KYC, Kuzmenko I, Kale GM, Gidalevitz D (2006) *Biophys J* 90:1275–1287.
52. Als-Nielsen J, McMorrow, D (2002) *Elements of Modern X-ray Physics* (Wiley, New York), Vol 43.
53. Ramamoorthy A, Thennarasu S, Lee DK, Tan A, Maloy L (2006) *Biophys J* 91: 206–216.
54. Burkoth TS, Fafarman AT, Charych DH, Connolly MD, Zuckermann RN (2003) *J Am Chem Soc* 125:8841–8845.